Thus it is seen from (18a) and (18c) that

$$K_f \to \frac{M^4}{(M^2-1)^{1/2}}\,\theta + 0\left(\frac{1}{A}\right)\theta'$$

$$K_f' \to -\frac{M^4}{(M^2-1)^{1/2}}\,\theta' + 0\left(\frac{1}{A}\right)\theta$$

The first terms are exactly the same as for weak shocks in ordinary gasdynamics. Hence, the fast shocks become ordinary gas shocks. The second terms indicate that the coupling between the upper and lower flows weakens toward zero as $A \to \infty$.

The slow waves also weaken (i.e., $\delta\rho_s/\rho \to 0$, etc.) as $A \to \infty$. However, as the angle ω_s tends to zero, θ and θ' must decrease correspondingly in order for linear theory to be applicable. If θ and θ' are held fixed, therefore, the result as $A \to \infty$ becomes meaningless. As already pointed out by Grad,[5] the slow wave collapses toward the body and becomes a thin region around it, in which the flow cannot be expected to tend to the gasdynamic limit. Such difficulties, of course, will not occur in the results of a nonlinear formulation.

Had $A < M$ been assumed instead of $A > M$, exactly the same behavior of the slow wave would occur as $M \to \infty$ and A remains fixed. Moreover, whether $M > A$ or $M < A$, analogous difficulties would occur with the fast wave as both M and A tend to infinity, but this is exactly similar to the hypersonic limit in ordinary gasdynamics, and one naturally should not expect the linear theory to hold.

References

[1] Bazer, J. and Ericson, W. B., "Oblique shock waves in a steady two-dimensional hydromagnetic flow," *Proceedings of Symposium on Electromagnetics and Fluid Dynamics of Gaseous Plasmas* (Polytechnic Institute of Brooklyn, Brooklyn, N.Y., 1962), pp. 387–414.

[2] de Hoffmann, F. and Teller, E., "Magneto-hydrodynamic shocks," Phys. Rev. **80**, 692–703 (1950).

[3] Friedrichs, K. O., "Non-linear wave motion in magnetohydrodynamics," Los Alamos Rept. LAMS-2105 (1954); revised and re-issued as New York Univ. Rept. NYO-6486-VIII (1958).

[4] Golitsyn, G. S., "Plane problems in magnetohydrodynamics," Soviet Phys.—JETP **7**, 473–477 (1958).

[5] Grad, H., "Reducible problems in magneto-fluid dynamic steady flows," Rev. Mod. Phys. **32**, 830–847 (1960).

[6] Helfer, L., "Magnetohydrodynamic shock waves," Astrophys. J. **117**, 177–199 (1953).

[7] Kiselev, M. I. and Kolosnitsyn, N. I., "The calculation of oblique shock waves in magnetohydrodynamics," Soviet Phys.—Doklady **5**, 246–248 (1960).

[8] Lüst, R., "Magneto-hydrodynamische Stosswellen in einem Plasma unendlicher Leitfahrigkeit," Z. Naturforsch. **8a**, 277–284 (1953).

[9] Lynn, Y. M., "Centered rarefaction waves in steady magneto-fluid dynamic flows," Bull. Am. Phys. Soc. **7**, 456 (1962).

[10] Lyubimov, G. A., "Stationary flow of an ideally conducting gas around a corner," Soviet Phys.—Doklady **4**, 529–531 (1959).

[11] McCune, J. E. and Resler, E. L., Jr., "Compressibility effects in magnetoaerodynamic flows past thin bodies," J. Aerospace Sci. **27**, 493–503 (1960).

MAY 1963 AIAA JOURNAL VOL. 1, NO. 5

Analysis of the Fluid Mechanics of Secondary Injection for Thrust Vector Control

JAMES E. BROADWELL*

Space Technology Laboratories Inc., Redondo Beach, Calif.

An analysis is made of the interaction of an injected gas or liquid with a supersonic stream, and the force induced on an adjacent wall is predicted. The study deals only with the free-stream-injectant interaction; the modifications to the flow introduced by the boundary layer are not considered. In the case of liquids, it is shown that the momentum deficit of the injectant relative to the freestream may play a larger part in producing the side force than the volume generation by vaporization and reaction. The analytical results are compared with those obtained from experiments in a wind tunnel and in nozzles.

Nomenclature

c = speed of sound
C_p = specific heat at constant pressure
E = energy per unit length
E_1 = energy per unit area
F_a = axial force or thrust, for exhaust to vacuum
F_i = interaction force
F_j = injection jet reaction force
F_m = maximum interaction force
F_w = wall force
F_T = axial force or thrust
F_s = side force
F_v = injection jet reaction force, for exhaust to vacuum
g = nondimensional pressure ratio
$\bar{g}$ = average nondimensional pressure ratio
$(I_{sp})_s$ = side specific impulse
J_0 = nondimensional constant
J_1 = nondimensional constant
K = amplification ratio, $(F_s/m_i)/(F_a/m_p)$
L = pressure field length
M = Mach number
m = mass flow
n = molecular weight
p = pressure
p_T = total pressure
r = radial distance
R = shock wave radius
$\bar{R}$ = gas constant
t = time
T = temperature

Received by ARS November 1, 1962; revision received February 18, 1963. This work was supported by Headquarters, Ballistic System Division, Air Force Systems Command, U. S. Air Force, under Contract No. AF 04(694)-1. The author wishes to acknowledge many helpful discussions during the course of this work with A. G. Hammitt and Hans W. Liepmann.

* Associate Manager, Aerosciences Laboratory Research Staff. Member AIAA.

T_T = total temperature
U = shock speed
u = x direction velocity
V = velocity
V_j = injection jet velocity
$(V_j)_e$ = injection jet effective velocity
$(V_j)_v$ = injection jet effective velocity, for exhaust to vacuum
$(V_{ex})_v$ = primary stream exhaust velocity, for exhaust to vacuum
w = injection mass flow per unit area
x = distance in primary stream direction
α = angle between injection nozzle axis and primary nozzle axis
β = angle between normal to nozzle wall and primary nozzle axis
γ = ratio of specific heat, primary stream
ϵ = primary nozzle area ratio
η = ratio r/R
θ = circumferential angle, measured from injection plane
ρ = density

Subscripts

i = injectant
j = injection jet
p = primary stream
∞ = freestream or primary stream

1. Introduction

THE practicality of changing the thrust direction of a rocket engine by injecting a gas or liquid into the nozzle is now well established,[1] but the fluid mechanical processes involved still are not well understood. It is the purpose of this paper to present some partly new concepts of these processes and to compare the predictions of a preliminary analysis, based on these ideas, with experiment.

Control of the thrust vector direction is achieved by an arrangement such as is sketched in Fig. 1. Gas, or a liquid that vaporizes, is injected into the nozzle downstream of the throat, creating a disturbance and an accompanying increase in force on the wall. This force, called the *interaction force*, acts mainly in the lateral direction but usually also causes a small increase in thrust. This induced force acts in addition to the direct reaction from the fluid injection.

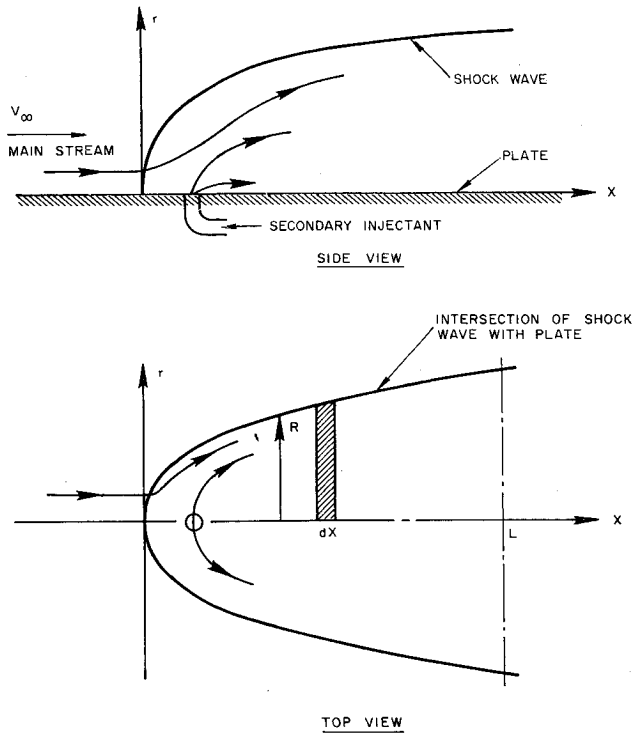

Fig. 1 Secondary injection flow pattern

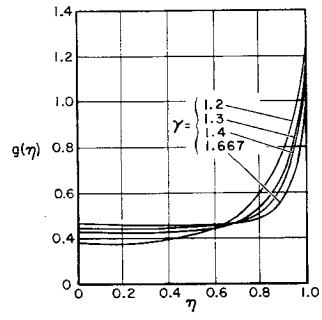

Fig. 2 Nondimensional pressure in cylindrical explosion (after Sakurai)

This paper deals with the interaction of the injected, or secondary, fluid with the primary freestream; the boundary layer on the nozzle wall is ignored. The boundary layer, of course, makes important modification to the flow, but the results obtained suggest that many of the essential features of the injection process are contained in the "inviscid" analysis. In any case, an understanding of the freestream-injectant interaction would provide a basis for a more general study, including the effects of the boundary layer.

Although the aim of the analysis is the description of the important aspects of the interaction processes and the discovery of the parameters controlling them, the results, combined with a single constant taken from experiment, appear to be directly useful in their present form.

2. Analysis

As an initial step in the analysis, consider the problem of determining the interaction force acting normal to a plane infinite wall when a gas or liquid is ejected from a single hole in the wall into an adjacent semi-infinite supersonic flow of a perfect gas. It is considered that the injected fluid constitutes a source of mass, momentum, and energy in the primary stream adjacent to the wall and that the pressure field created by the source causes the side force. If the boundary layer on the wall is ignored, then the wall is a plane of symmetry, and the changes in the primary flow caused by the source are the same as those produced in an infinite stream.

2.1. The Effect of Momentum Deficit

Now assume that in the forementioned situation the injected liquid has thermodynamic characteristics such that its vaporization and mixing with the primary stream causes no net volume change, i.e., that the mixing of injectant and freestream gas at constant pressure is a constant volume process. (It will be shown later that this condition is not only useful to simplify the start of the analysis but is of practical interest as well.) Under these conditions and at sufficiently high Mach number, blast wave theory[2] should give an adequate description of many aspects of the flow. In particular, it is expected intuitively that the force on the wall would be one of the quantities given most accurately. On the other hand, the pressure distribution in the immediate neighborhood of the port is not correct.

The blast wave theory, which is based on an analogy between the cylindrical unsteady flow produced by the explosion of a line charge and axially symmetrical steady flow, has been applied to the flow about blunt bodies at hypersonic and high supersonic speeds.[2] The flow field is determined by the energy added per unit length of gas, a quantity that, in the usual applications of the theory, is equal to the drag of the body under consideration. In the present case, the injected fluid mixes with the freestream, accelerates to the freestream velocity, and thus, if it enters with zero axial momentum, exerts an effective force on the primary stream equal to $m_i V_\infty$, where m_i is the rate of secondary injection and V_∞ the freestream velocity. This assumption, that the injected fluid attains freestream velocity, replaces the detailed analyses of

Wu, Chapkis, and Mager[3] and Ferrari,[4] involving the assumption that the injectant expands to the ambient pressure without mixing. In Appendix A the injectant momentum deficit is treated within the framework of linearized theory, and a comparison with the corresponding results of Ref. 3 is made.

The force on the wall and the locus of the shock wave generated by the injection are determined as follows. Begin with the shock wave and pressure field generated by the explosion of a line charge. The first-order solution, valid when the shock is strong, is given by Sakurai[5] and by Sedov[6] in the form

$$(c/U)^2(R_0/R)^2 = J_0(\gamma) \tag{1}$$

$$(p/p_\infty)(c/U)^2 = g(\eta) \tag{2}$$

where c is the sound speed in the undisturbed fluid, R the shock position, $U = dR/dt$ the shock speed, J_0 a constant depending on the ratio of specific heats γ, p the pressure, $\eta = r/R$ with r the distance from the center of the explosion, and R_0 is defined by

$$R_0 = (E/2\pi p_\infty)^{1/2} \tag{3}$$

with E the energy per unit length released in the explosion. The function $g(\eta)$ is given in Fig. 2 for several values of γ. Solution of Eq. (1) yields

$$R = (2cR_0/J_0{}^{1/2})^{1/2}\, t^{1/2}$$

Now, in accord with the analogy between this flow and axially symmetric hypersonic flow, replace t by x/V_∞ and, letting $R^* = R/R_0$ and $x^* = x/R_0$, then one obtains

$$R^* = (2^{1/2}/J_0{}^{1/4})M_\infty{}^{-1/2}(x^*)^{1/2} \tag{4}$$

where M_∞ is the freestream Mach number. The pressure is given by

$$p/p_\infty = (1/2J_0{}^{1/2})M_\infty g(\eta)(x^*)^{-1} \tag{5}$$

Next consider that the energy is released adjacent to a wall, as indicated in Fig. 1, and compute the wall force by

$$F_w = 2\int_0^L \int_0^R (p - p_\infty)drdx =$$

$$2p_\infty \int_0 \int_0^R \frac{p}{p_\infty}\, drdx - 2p_\infty \int_0^L \int_0^R drdx \tag{6}$$

where L is for the moment an arbitrary length. Introducing the expressions for R^* and p/p_∞ from Eqs. (4) and (5) and the definition of R_0 from Eq. (3), one obtains

$$F_w = \frac{2E}{\pi}\left[\frac{1}{2^{1/2}J_0{}^{3/4}}\,\bar{g}M_\infty{}^{1/2}(L^*)^{1/2} - \frac{2^{1/2}}{3J_0{}^{1/4}}\,M_\infty{}^{-1/2}(L^*)^{3/2}\right] \tag{7}$$

where

$$\bar{g} = \int_0^1 g(\eta)d\eta \qquad L^* = L/R_0$$

It is difficult to make a definite choice for L^*. Equation (7) contains a maximum F_w as a function of L^*, and it is assumed in the following that L^* is the value that yields this maximum force. The use of this value for L^* corresponds to the assumption that there is sufficient length downstream of the injection port for the maximum force to be realized but that the plate or nozzle is not so long as to cancel part of the generated side force. Fortunately, as is pointed out later, the side force is a slowly varying function of L^* in the neighborhood of the maximum, and the choice of L^* is less critical than appears here. The value of L^* for maximum F_w is

$$L_m{}^* = \bar{g}M_\infty/2J_0{}^{1/2} \tag{8}$$

and the maximum force F_m is

$$F_m = (2\bar{g}^{3/2}/3\pi J_0)EM_\infty$$

Figure 2 shows that $\bar{g}$ is approximately $\frac{1}{2}$, independent of γ, and, according to Sakurai, $J_0(1.2) = 1.55$ and $J_0(1.4) = 0.88$. Finally, remembering that E is the energy per unit length in the completely symmetrical case, and that in the present problems all the energy is confined to the space above the plane, set $E/2$ equal to the drag,† m_iV_∞, to get

$$F_m = \sigma(\gamma)M_\infty V_\infty m_i \tag{9}$$

where

$$\sigma(1.2) = 0.10 \qquad \sigma(1.4) = 0.17 \tag{10}$$

At this point, a remark about the accuracy of the first-order blast wave solution is required. When the expression for $L_m{}^*$, Eq. (8), is substituted for x^* in Eq. (5), the result is $p/p_\infty = 2g(\eta)$. Thus at $L_m{}^*$ the pressure ratio across the shock has dropped to approximately 2, and the first-order theory is inaccurate in this region.[7] Examination of Eq. (7) reveals, however, that a large part of the force is realized near the origin; in fact, F_w has reached approximately 70% of its maximum value at $x^* = \frac{1}{4}L_m{}^*$. Thus, especially in view of the preceding approximations, the first-order results seem sufficient for the present purpose.

As mentioned earlier, the insensitivity of the force to L is also somewhat of a justification for the rather arbitrary use of L_m as the downstream limit of integration in Eq .(6).

2.2. Effect of Volume Addition

In this section the preceding analysis is generalized to allow volume as well as drag to be added by the source. To see that this is an additional effect, consider a case in which gas already at freestream velocity (in direction as well as magnitude) is the injectant. Again the primary stream will be deflected to make room for the added gas and a pressure field generated.

To account for this volume addition, in an approximate way, proceed as follows. The injected gas, after attaining the velocity V_∞, will occupy a given volume per unit length. The effect of this steady creation of volume can be simulated by heat addition to the primary stream. The advantage of this point of view is that the blast wave theory again can be applied with the energy per unit length required for the volume generation added to that coming from the drag.

Let heat be added to a portion of the primary flow, m_c, at such a rate that the resulting change in volume is equal to the added volume, with all processes taking place at the constant pressure p_∞. That is, let

$$(m_c/\rho_2) - (m_c/\rho_\infty) = m_i/\rho_i \tag{11}$$

where ρ_i is the density of the injected gas at p_∞ and with a temperature equal its total temperature at injection,‡ and ρ_2 is the downstream density in the heated stream tube.

Assuming the freestream to be a perfect gas and letting $s = m_c/m_i$, one obtains

$$T_2 = (p_\infty/s\rho_i\bar{R}_\infty) + T_\infty$$

where $\bar{R}_\infty$ is the freestream gas constant. Applying the energy equation to the flow between a station far upstream and station 2, and noting that the velocity is constant from momentum considerations, one has

$$Q = C_{p\infty}(T_2 - T_\infty)m_is = C_{p\infty}(p_\infty/\rho_i\bar{R}_\infty)m_i \tag{12}$$

† See Appendix B for a further discussion of the relation between energy and drag.

‡ The injected fluid is assumed, in accord with the ideas discussed earlier, to expand without doing work to p_∞, i.e., the lateral velocity it attains in the injection nozzle is lost when it mixes with the freestream.

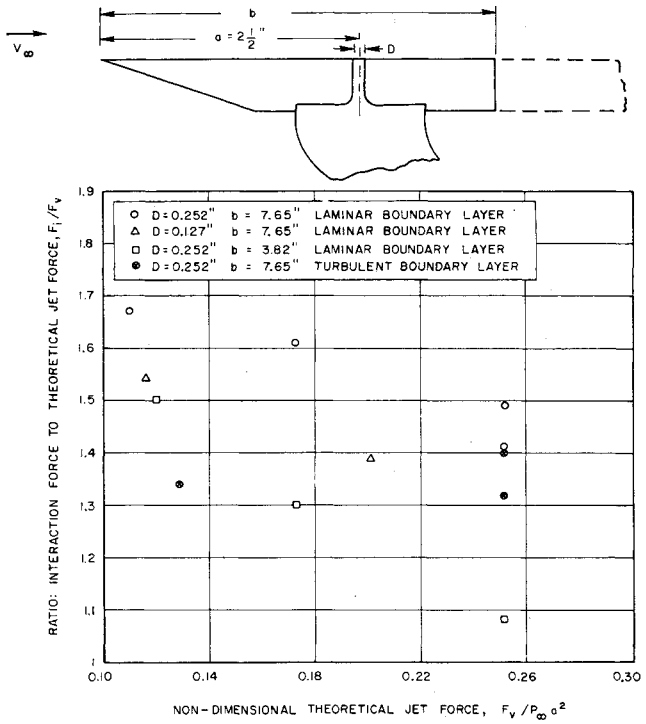

Fig. 3 Normal force due to side jet interaction on flat plate, $M_\infty = 3.85, p_\infty = 0.1146$ psia[9]

independent of s. Thus, the increased energy per unit length in the present problem is

$$2C_{p\infty}(p_\infty/\rho_i\bar{R}_\infty)(m_i/V_\infty)$$

and the total energy can be written as

$$E = 2m_iV_\infty\left[1 + \frac{1}{(\gamma - 1)M_\infty^2}\frac{\rho_\infty}{p_i}\right]$$

With this new expression for E, Eq. (9) becomes

$$F_m = \sigma(\gamma)M_\infty V_\infty\left[1 + \frac{1}{(\gamma - 1)M_\infty^2}\frac{\rho_\infty}{\rho_i}\right]m_i \quad (13)$$

When the injectant is a perfect gas, it is convenient to write Eq. (13) in the form

$$F_m = \sigma(\gamma)M_\infty V_\infty\left[1 + \frac{2 + (\gamma - 1)M_\infty^2}{2(\gamma - 1)M_\infty^2}\frac{n_\infty}{n_i}\frac{T_{Ti}}{T_{T\infty}}\right]m_i \quad (14)$$

in which $T_{T\infty}$, n_∞, T_{Ti}, and n_i are the total temperature and molecular weight of the freestream and the injectant, respectively. The application of these volume corrections to reactive fluids is discussed in Sec. 4.

Perhaps it is not unexpected, in view of the approximations in the analysis and the neglect of the boundary layer, that Eqs. (13) and (14) fail to predict the magnitude of the side force accurately. In anticipation of this result, a constant C, to be determined by experiment, is introduced into these equations as a multiplying factor:

$$F_i = C\sigma(\gamma)M_\infty V_\infty\left[1 + \frac{1}{(\gamma - 1)M_\infty^2}\frac{\rho_\infty}{\rho_i}\right]m_i \quad (15)$$

and

$$F_i = C\sigma(\gamma)M_\infty V_\infty\left[1 + \frac{2 + (\gamma - 1)M_\infty^2}{2(\gamma - 1)M_\infty^2}\frac{n_\infty}{n_i}\frac{T_{Ti}}{T_{T\infty}}\right]m_i \quad (16)$$

where F_i now denotes the predicted interaction force.

2.3. Two-Dimensional Flow

It is clear that the foregoing analysis can be applied to the two-dimensional problem, i.e., to the case in which the injectant enters through a slot in the wall. The result is

$$F_m = \tfrac{4}{3}[g_1(0)]^{3/2}(M_\infty/J_1)E_1$$

where E_1 is the energy per unit area of the explosion, and $g_1(0)$ and J_1 are constants depending on γ. Again using the values of Sakurai,

$$g_1(0) = 0.42 \qquad J_1 = 3.02 \qquad \gamma = 1.2$$
$$g_1(0) = 0.47 \qquad J_1 = 1.7 \qquad \gamma = 1.4$$

one gets

$$F_m = 0.12\,M_\infty E_1 \qquad \gamma = 1.2 \quad (17)$$
$$= 0.25M_\infty E_1 \qquad \gamma = 1.4 \quad (18)$$

These equations show that injection is approximately three times more effective when the injectant enters through a slot (and the resulting flow is two-dimensional) than when it enters at a point.

2.4. Direct Reaction from the Injection

The aim of the foregoing sections is the prediction of the side force arising from the interaction of the injected fluid and the primary stream. It usually is assumed that the total side force is made up of this force plus the direct reaction force from the injection. However, the fact that at least some of the lateral injection momentum is absorbed by the primary stream within the nozzle raises a question as to whether this additional side force actually is realized. Although the question can be answered only by experiment, and the formulation of a critical experiment is not easy, it is assumed in the following that in the distance available a negligible portion of the injection momentum is transmitted to the walls. Thus the total side force is taken to be the sum of the interaction force of the preceding sections and the injection jet reaction force.

3. Comparison with Gas Injection Experiments

The most extensive set of experiments with which the present analysis can be compared are those reported by Rodriguez[8] dealing with the injection of air into air nozzles and the injection of cool gas into LOX-RP1 nozzles. Preceding an examination of these results, however, is a discussion of experiments performed in the University of Michigan wind tunnel in which air was ejected from a flat plate.

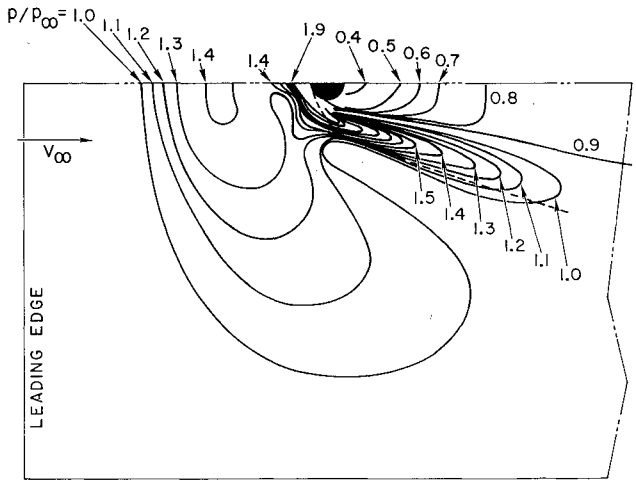

Fig. 4 Flat plate pressure distribution, 0.252-in.-diam sonic nozzle, $(p_T)_j/p_\infty = 22.5$, $M_\infty = 3.69$, laminar boundary layer[9]

3.1. University of Michigan Flat Plate Experiments

Amick and Hays[9] present pressure distributions and forces on a flat plate in a supersonic wind tunnel when air is ejected from variously shaped nozzles with exit planes flush with the plate. A large portion of their investigation deals with the effect of plate size on the force, and hence many of their data were taken when part of the region of increased pressure was off the plate. However, one of the authors[15] kindly has furnished a set of data in which force measurements that are not influenced by the plate width can be identified. Figure 3 is a plot of a portion of these measurements. F_i is the measured interaction force, i.e., the increase in normal force on the plate due to the jet minus the jet reaction force, and F_v is the theoretical jet force for exhaust into a vacuum. This latter force is given by

$$F_v = m_i(V_j)_v = V_j[1 + (1/\gamma M_j^2)]m_i$$

where $(V_j)_v$ is the effective exhaust velocity in vacuum, V_j the jet velocity, and M_j the jet Mach number. Thus, making use of Eq. (16) with $T_{T_i} = T_{T\infty}$ and $n_i = n_\infty$, one obtains

$$\frac{F_i}{F_v} = \frac{C\sigma(\gamma)M_\infty V_\infty}{(V_j)_v}\left[1 + \frac{2 + (\gamma - 1)M_\infty^2}{2(\gamma - 1)M_\infty^2}\right]$$

$$= 1.35C$$

at $M = 3.85$ and for a sonic injection nozzle.

At low injection rates (low F_v) and with the longer plate ($b = 7.65$ in.), the measured force ratio varies only little with $F_v/p_\infty a^2$ and is approximately independent of jet diameter. Estimating the average value of F_i/F_v at the lowest rate to be approximately 1.6 yields a value for C of 1.2. That this value is of order 1 is some support for the validity of the preceding approximations.

The decrease of F_i/F_v with increasing injection rate, especially noticeable with the shorter plate, is in qualitative agreement with the analysis in the following sense. If the plate length is shorter than L_m, then the force decreases as the plate length decreases. Hence, since L_m increases with m_i, the ratio F_i/F_v falls with increase of this variable. Quantitatively, however, the measured force begins to fall at a much lower value of m_i than is predicted by the analysis.

A typical pressure distribution given in Ref. 9 is shown in Fig. 4. The contours are lines of constant pressure and were obtained by interpolation between the many measured values.

The dotted line marks the intersection of the shock wave with the plate according to the analysis. Although the proximity of this line to the measured ridge of high pressure is encouraging, its importance should not be overemphasized. There are two reasons for the qualification: first, shock shape is not sensitive to the flow behind it, and second, the origin of the shock is not fixed precisely in the blast wave theory. Perhaps of more significance is the qualitative agreement between analysis and experiment in the shape of pressure traces in lateral planes downstream of the port. The downstream pressure on an axial line through the port center, however, rises with x in the experiment but approaches ambient from above in the theory. There is, again, agreement in the x-behavior of the maximum pressure.

It is seen that boundary layer separation spreads the pressure field over an area much larger than that enclosed by the shock wave. Interestingly enough, however, no consistent effect of the boundary layer state, laminar or turbulent, on the measured side force was observed. The pressure distribution is changed considerably, however.

Amick and Hays find that the pressure field induced on the plate by a small circular cylinder attached to the plate is quite similar to that shown in Fig. 4, a result that lends support to the idea that flow with injection is like that about a blunt body creating drag.

3.2. Rocketdyne Nozzle Experiments

The experiments reported in Ref. 8 consisted of a thorough survey of wall pressures in nozzles with area ratios of 25 and 16 to 1 with secondary injection at the throat and downstream of the throat. Both primary and secondary fluids were air at room temperature. Also measured were side and axial forces in a LOX-RP1 engine when the injectant was a mixture of LOX and RP1 in various proportions. (Throat injection, which caused little or no side force, will not be discussed further.) In all cases the injection was through circular convergent nozzles providing sonic flow. Most of the measurements were for single nozzles with axes normal to the local nozzle wall, but tests also were run at injection angles of 30° upstream and downstream from the normal to the wall and with multiple nozzles.

Several parameters are used to describe the performance of injection systems: 1) the ratio of side force to axial force or thrust, F_s/F_a, the thrust being the value with zero injection and for exhaust to vacuum; 2) the amplification factor K defined as $K = (F_s/m_i)/(F_a/m_p)$, where m_p is the primary flow rate; 3) the ratio of the increase in axial force, ΔF_a, to thrust.

To apply the results of the earlier section in the evaluation of these parameters, a restriction and modification, both connected with the nozzle geometry, are required. First, the injection rates must be low; otherwise the orientation of each wall element on which the increased pressure acts would have to be taken into account. Such effort is not warranted, at present, primarily because the influence of the boundary layer on pressure distribution is not accounted for in the analysis. For the same reasons no attempt has been made to compute the side force for injection near the nozzle exit.

At the low flow rates, the induced and direct forces must be resolved into their lateral and axial components, a modification determined by the wall slope at the point of injection and the injection nozzle angle. Hence one has, making use of Eq. (16),

$$\frac{F_s}{F_a} = 1.2\sigma(\gamma)M_\infty \frac{V_\infty}{(V_{ex})_v}\left[1 + \frac{2 + (\gamma - 1)M_\infty^2}{2(\gamma - 1)M_\infty^2}\frac{T_{T_i}}{T_{T\infty}}\right] \times \sin\beta\,\frac{m_i}{m_p} + \frac{(V_j)_e}{(V_{ex})_v}\sin\alpha\,\frac{m_i}{m_p} \quad (19)$$

where 1) the value of $C = 1.2$ is retained; 2) $(V_{ex})_v$ and $(V_j)_e$ are the primary and injection effective exhaust velocities, respectively, with the primary exhausting to vacuum; 3) β is the angle between the normal to the nozzle wall at the point of injection and the primary nozzle axis; 4) α is the angle between the injection nozzle axis and the primary nozzle axis; and 5) the subscript ∞ now indicates primary flow conditions at the injection station.

In the air nozzle tests the primary and secondary supply temperatures had a common value equal to ambient temperature, and $T_{T_i}/T_{T\infty}$, was unity. Thus with $\sigma(\gamma) = 0.17$ and the assumption that the primary flow is one-dimensional, F_s/F_a can be evaluated at each injection station. The increase in axial force is given by Eq. (19) with the sine replaced by the cosine. The other performance parameters also come directly from Eq. (19).

Some comparisons between the experimental and analytical results for the 25:1 nozzle§ appear in Figs. 5–9. The agreement between the analytical and experimental side forces is satisfactory at low flow rates except for injection downstream of $\epsilon = 17$. The proximity to the nozzle exit plane almost certainly explains this disagreement. The independence of the forces from injection port size and hence injection pressure is another important point of agreement, as is the slight rise of amplification factor with ϵ or M_∞ upstream of $\epsilon = 17$.

A comparison of Figs. 5 and 8 strongly suggests that the major cause of the decrease in amplification factor (the slope

§ A description of this and the other nozzle appears in Ref. 8.

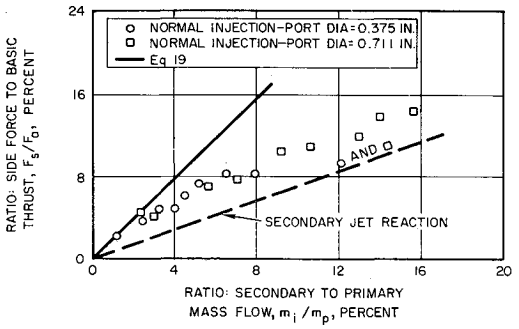

Fig. 5 Variation of side force with secondary mass flow for injection at ϵ = 12.8:1 in 25:1 nozzle, cold flow test (experimental data from Ref. 8)

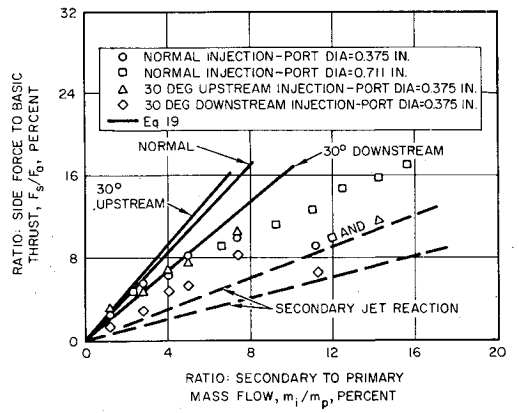

Fig. 6 Variation of side force with secondary mass flow for injection at ϵ = 17.1:1 in 25:1 nozzle, cold flow test (experimental data from Ref. 8)

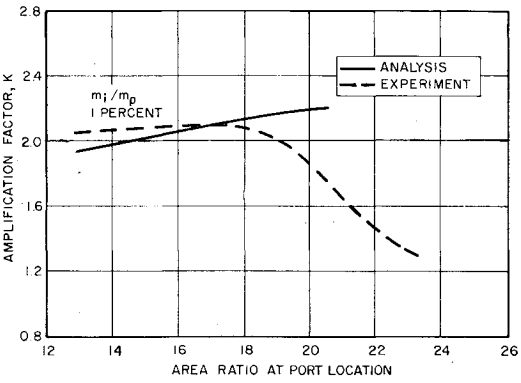

Fig. 7 Variation of amplification factor with port location for 25:1 nozzle, cold flow test (experimental data from Ref. 8)

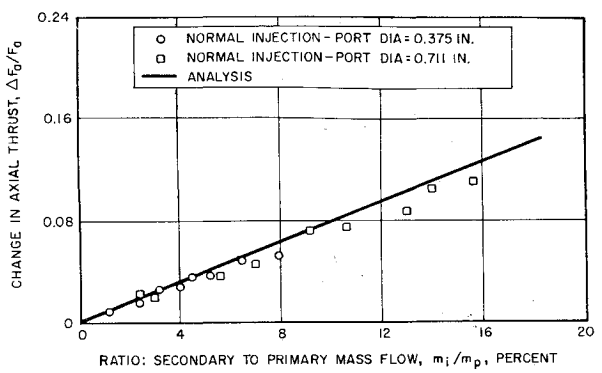

Fig. 8 Change in axial thrust with secondary mass flow for injection at ϵ = 12.8:1 in 25:1 nozzle, cold flow test (experimental data from Ref. 8)

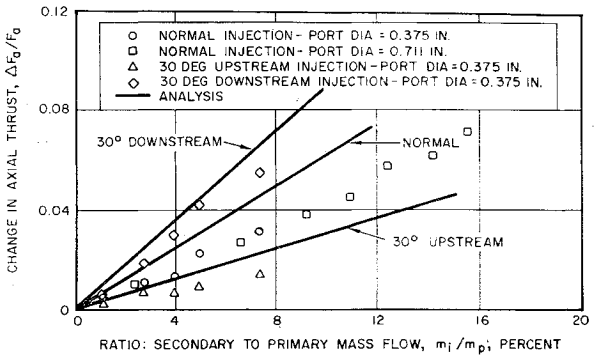

Fig. 9 Change in axial thrust with secondary mass flow for injection at ϵ = 17.1:1 in 25:1 nozzle, cold flow test (experimental data from Ref. 8)

of the F_s/F_a vs m_i/m_p curve) with flow rate is the expansion of the increased pressure region circumferentially from the injection port.

The agreement between the analysis and experimental data for the 16:1 nozzle is similar to that just discussed. The details appear in Ref. 10.

Tests also were carried out in two nozzles in which LOX-RP1 was the primary stream, and the injectant was composed of the same substances at various mixture ratios and hence temperatures. The limited results at low flow rates were in approximate accord with Eq. (19), which predicts a large drop in the ratio F_s/F_a for three reasons: 1) $\sigma(\gamma)$ decreases from 0.17 to 0.10; 2) $T_{Ti}/T_{T\infty}$ is reduced greatly; and 3) the ratio $(V_j)_e/(V_{ex})_v$ falls as the square root of $T_{Ti}/T_{T\infty}$. Again, the details of the comparison between the analysis and experiment appear in Ref. 10.

4. Liquid and Reactive Fluid Injection

For the foregoing analysis to be applicable in its present form to liquid and to reactive fluid injectants, vaporization and reaction times must be short compared with the time a given injectant particle remains within the nozzle. The establishment of criteria for meeting this condition is an important problem but one that will not be studied here; instead it will be assumed, as some indirect evidence indicates, that fluids of interest react in short enough times in actual, high-temperature propellants.

When vaporization and reaction occur, the factor ρ_∞/ρ_i in Eq. (15) is not well defined. It will be treated in the following way. The injectant is assumed to mix and react at constant pressure with the primary stream (with the primary gas initially at its local static temperature) and the *net change* in volume, per unit mass of injectant computed. Then, since effectively each unit mass injected brings about this volume change in the system, the reciprocal of the volume change is set equal to ρ_i. The values of ρ_∞/ρ_i for Freon 114B-2, LOX, and water, three suggested injectants, in a typical solid propellant are shown in Fig. 10 as a function of mixture ratio, i.e., as a function of the mass of injectant per mass of propellant.[‖] Note that this mixture ratio is not the ratio of secondary to primary mass flow because the mixing is, by design, not uniform.

One sees that the Freon causes little volume change compared to the propellant specific volume and that the addition of water causes a net *loss* in volume. This latter result is not unexpected in view of the energy required to vaporize and to raise the temperature of the water to that of the mixture.[#]

[‖] The analysis and calculations yielding these results were made by Leslie Van Nice of the Propulsion Research Department.

[#] In the analysis of Ref. 3 applying to liquid injection, only the volume increase of the injectant was considered. It also should be noted that the linearized analysis applied there will yield zero side force when injection causes no net volume change. See Appendix A for a discussion of this point.

Likewise, the large increase in volume produced by LOX injection is understood easily.

Experimental data for LOX injection are not yet available, but Newton and Spaid[1] have made extensive measurements of pressure distribution and side force for Freon 12 injection in small solid propellant engines and a few measurements with water and nitrogen. The volume effects of the reaction of Freon 12 and water with their propellant should be similar to that shown in Fig. 10, so that a comparison of their measurements with analytical results using values of ρ_∞/ρ_i from Fig. 10 is worthwhile. Fortunately, the change in volume associated with Freon and water injection is relatively insensitive to the mixture ratio, for this quantity may be difficult to estimate.

The nozzles used in the experiments of Ref. 1 were conical with 15° half-angles, had 25:1 expansion ratios, were about 11 in. long, and had throat diameters of 1.41 in. All the experimental data referred to in this section were taken in these nozzles.

The measured pressure distributions for Freon and nitrogen injection are, except in the region immediately downstream of the injector, remarkably alike and are, again excepting the neighborhood of the injector, similar to those predicted by the blast wave theory. They also show clearly the loss in effectiveness of pressure increases out of the injector plane.

Figure 11 illustrates the rise in side specific impulse, $(I_{sp})_s = F_s/32.2m_i$, with axial length downstream of the injection port. The curves represent the values of the pressure integrals to successive downstream stations, the analytical curve being obtained from the force realized on various lengths short of L_m, equal in this case to about 2 in. The analytical curve begins at a value equal to the I_{sp} produced by the injection momentum; the experimental starting value includes this contribution as well as the small amount arising from pressure increase upstream of the injector. The final value attained by the analytical curve exceeds the experimental, because the former is uncorrected for nozzle wall curvature, an effect that is considerable at this injection rate. Again, as was suggested by the Rocketdyne and Michigan experiments, the analytical region of increased pressure is too short.

Figures 12 and 13 contain analytical and experimental values of the side force-axial thrust ratio as a function of mass flow ratio, the experimental results in this case coming from thrust stand measurements.

In the analysis it was assumed that the primary stream was a perfect gas with $\gamma = 1.2$ and that the nozzle throat velocity was 3500 fps. With these assumptions, C set equal to 1.2 as before, and ρ_∞/ρ_i from Fig. 10, Eq. (15) yields the interaction force** as a function of injection rate m_i. It may be noted here that the volume term in Eq. (15) contributes only about 15% of the side force. Also, as mentioned previously, the analytical curves, being uncorrected for nozzle wall curvature, are applicable only at low flow rates. In addition to flow rate, injector diameter and injection angle relative to the wall were varied in the experiments. Both of these parameters might be expected to influence the jet breakup and hence the fluid vaporization rate. The analysis assumes, as was stated earlier, that the fluid vaporizes completely at the injection station, and thus the single curve applies to all conditions. (The contribution of the injection momentum changes with angle and injection pressure, but the effect is small.) Although the amount of data at the low flow rates is limited, they show that the assumption may be a fair approximation.

The data in Figs. 12 and 13 were taken with the injector located at an area ratio ϵ of 8.81 and indicate the side specific impulse at low flow rates and zero injection angle to be in the

** This quantity multiplied by the cosine of the nozzle half-angle and added to the injection momentum is the side force. In Figs. 12 and 13 this force is shown divided by the axial thrust F_r instead of the thrust for exhaust to vacuum F_a of the earlier sections.

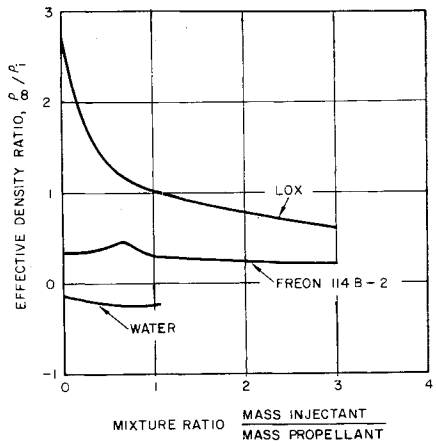

Fig. 10 Effective density ratio of injectants mixed with typical solid propellant exhaust expanded to 14.7 psia

range from 100 to 120 sec compared with an analytical value of 118 sec. With the injector located at an ϵ of 2.65, both the experimental and analytical values dropped to about 80 sec, again at low flow rates, i.e., $m_i/m_p \approx 0.05$. This drop is attributed in Ref. 1 to impingement of the shock wave on the wall opposite the injector, a statement that is based on pressure measurements at much higher flow rates, $m_i/m_p \approx 0.18$. An approximate calculation of the shock location by the blast wave theory shows that at the lower rates impingement would not occur, but that it almost happens at the higher rate. Thus the experimental evidence is not inconsistent with the analytical explanation that the decrease in performance is due to the lower Mach number and velocity at the injection station.

The two runs in which cold nitrogen was the injectant yielded $(I_{sp})_s$ of 181 and 161 sec compared with an analytical value of about 160 sec. This increase in performance over that of Freon is all due, according to the analysis, to the increased injection momentum. This conclusion does not seem to be substantiated by the measured pressure distributions that indicate a higher interaction force as well for the nitrogen.

The $(I_{sp})_s$ of water was measured in two runs to be 33 and 45 sec, whereas the analytical value was 96 sec. An obvious possible explanation for the difference is that the water is not vaporizing and accelerating to the primary stream velocity within the nozzle, but there is no direct evidence to support this conjecture.

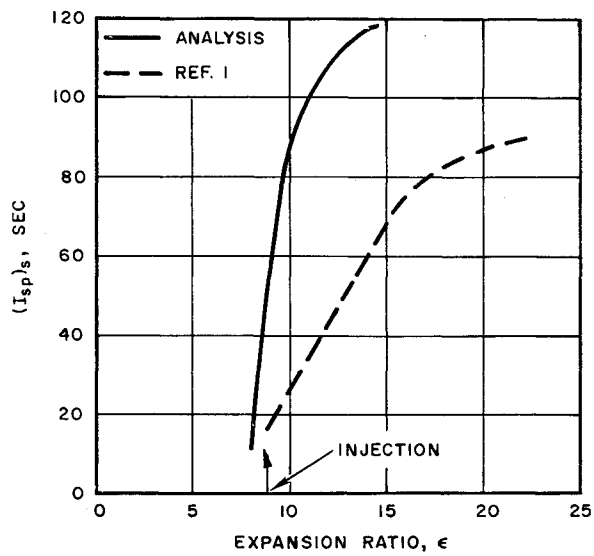

Fig. 11 Dependence of side impulse on axial distance with Freon 12 as injectant

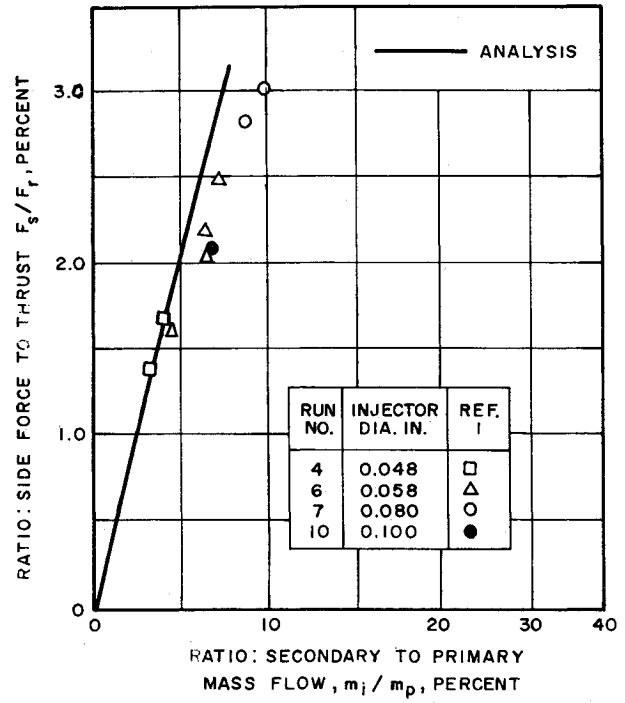

Fig. 12 Variation of side force with secondary mass flow for Freon 12 injection at $\epsilon = 8.81$; injection normal to nozzle wall

Finally a measurement was made of the side force induced by a solid plug attached to the nozzle wall. The measured value was about 3.5 lb ± 1 lb. Estimating the frontal area of the plug to be about 0.2 in.^{2} and taking the drag coefficient to be unity, the drag of the body is found to be about 7 lb. Setting E in Eq. (9) to twice this value, a side force of about 2.3 lb is computed. This order of magnitude agreement substantiates further the similarity noted in the Michigan experiments between the effects of fluid injection and the drag produced by a solid body.

5. Conclusions

A model has been developed of the interaction between an injected fluid and a supersonic freestream. It is based on the idea that the injected fluid acts as a source of mass, momentum, and energy in the primary stream and that the effects of the source are, to a large extent, independent of the wall boundary layer. This latter statement implies, of course, that the injection rate is to be high relative to the local mass flux in the boundary layer. When the source is concentrated at a point, an idealization of the injection of gas (or fluid that vaporizes quickly) from a single port, the resulting flow is analyzed by means of blast wave theory. Linearized theory is applied when the source is distributed.

A much more thorough comparison of analytical and experimental results is required before the correctness of the ideas and many assumptions involved in the model can be considered as established.†† The areas of agreement between the forementioned experiments and the analysis seem large enough to encourage this further investigation. In summary, 1) the pressure distributions on a flat plate and in nozzles for both liquid and gas injection are qualitatively in accord with those of the blast wave theory; 2) the magnitude of the side force induced by air (or nitrogen) injection in both cold and hot firings, by Freon injection in hot firings, and by a solid body is given approximately by the analysis; 3) although the Mach number dependence of the side force is not unequivocally established by the experiments, the evidence supports the analysis; and 4) the independence of the side specific impulse of air from injection total pressure, over the range tested, is an important check on the assumptions concerning the expansion and mixing processes.

The low performance of water, compared to that predicted, shows the need for further study. Another shortcoming of the analysis, probably attributable to the neglect of the boundary layer, is its failure to predict the correct size of the high pressure region.

In conclusion, it may be noted that, although the application of the analysis has been to the flow in rocket engine nozzles, it also is suitable to the study of control jets external to high speed vehicles.

†† A new set of experimental results,[11] in which the injectants were inert gases of widely varying molecular weight, recently has become available. A comparison of the analysis with these results will be reported later.

Appendix A: Linearized Theory

The preceding analysis deals with configurations in which the injectant is introduced at a point (and the subsequent flow is axially symmetrical) or along a line transverse to the flow with the resulting flow two-dimensional. It is also of interest to allow the injectant to enter from a line parallel to the flow or from an area. These problems are amenable to analysis when the injection causes small disturbances and linearized theory applies. The following discussion is restricted to the two-dimensional problem that arises when the injectant enters from a planar strip transverse to the primary flow and infinite in one dimension. Furthermore, in the interest of brevity, the injectant is taken to be a gas with a density equal to that of the freestream.

The usual source solutions developed for thin airfoil theory are not applicable directly to the present problem, because implicit in these solutions is the assumption that the source material enters with a velocity in the x direction, u, equal to the freestream velocity. One wants the initial x velocity of the injectant to be zero. A direct solution to this problem has not yet been found, but a scheme that seems intuitively correct in the following. Inject the fluid with u equal to V_∞, and then remove the unwanted momentum by a body force in the minus x direction equal to the product of V_∞ and the mass rate

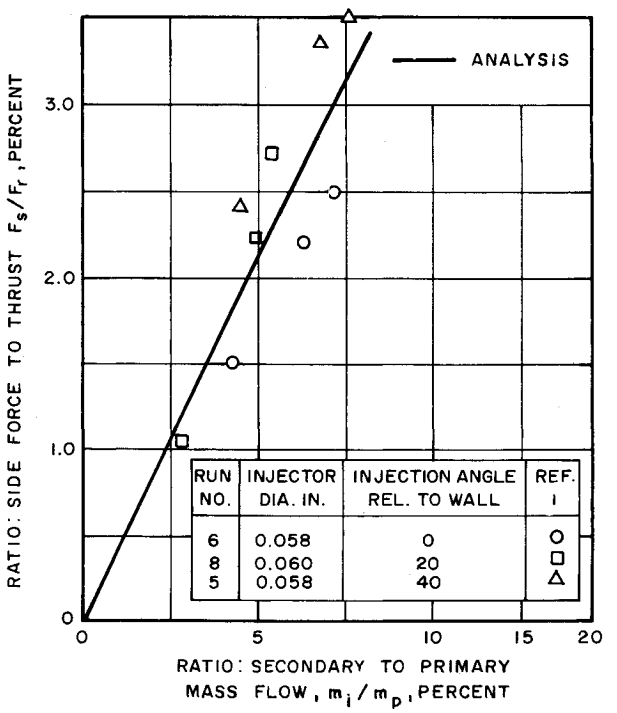

Fig. 13 Variation of side force with secondary mass flow for Freon 12 injection at $\epsilon = 8.81$; effect of injection angle

of injection.‡‡ Willmarth[13] has shown the effects in linearized flow of mass and heat sources and of body forces in the streamwise direction. A straightforward application of his results yields

$$p - p_\infty = \frac{V_\infty}{(M_\infty^2 - 1)^{1/2}} w + \frac{M_\infty^2}{(M_\infty^2 - 1)^{1/2}} V_\infty w$$

where w is the rate of mass addition per unit area. Only the first term in this expression appears in the linearized analysis in Ref. 3. The second term is seen to be of great importance even in the present problem in which the added mass has considerable volume (ρ_i was assumed to equal ρ_∞). As pointed out earlier, the first term may be negligible or even negative for some liquids.

Integration of the foregoing equation over the area of injection yields

$$F_i = [(1 + M_\infty^2)/(M_\infty^2 - 1)^{1/2}]V_\infty m_i$$

where F_i and m_i are, respectively, the interaction force and injection rate per unit length of strip. When $M_\infty^2 \gg 1$ (and changing the order of the terms),

$$F_i = [1 + (1/M_\infty^2)]M_\infty V_\infty m_i$$

a result that may be compared with the two-dimensional blast wave solution, modified to account for volume addition, contained in Eqs. (17) and (18):

$$F_i = 0.24\left[1 + \frac{1}{(\gamma - 1)M_\infty^2}\frac{\rho_\infty}{\rho_i}\right]M_\infty V_\infty m_i \qquad \gamma = 1.2$$

$$= 0.50\left[1 + \frac{1}{(\gamma - 1)M_\infty^2}\frac{\rho_\infty}{\rho_i}\right]M_\infty V_\infty m_i \qquad \gamma = 1.4$$

Since $\rho_\infty = \rho_i$,

$$F_i = [0.24 + (1.2/M_\infty^2]M_\infty V_\infty m_i \qquad \gamma = 1.2$$

$$= [0.50 + (1.25/M_\infty^2)]M_\infty V_\infty m_i \qquad \gamma = 1.4$$

Thus the dependence of the side force on the parameters M_∞, V_∞, and m_i is the same in the two approaches. Even more surprising and probably only fortuitious, the magnitude of the second or "volume" terms differs by only 20 or 25%, depending on γ. No attempt will be made here to examine the significance of the difference in magnitude of the momentum terms.

Appendix B

Putting energy per unit length equal to the drag requires further discussion when the drag is produced by injection, because this case differs in two essential ways from the blunt body flow. First, in the present situation, the injected mass absorbs energy, in the form of its own kinetic energy, in the amount $V_\infty^2/2$ per unit mass of injectant ($m_i V_\infty/2$ per unit length). Second, it is known that the presence of additional mass at the site of an explosion strengthens its effects. In fact, Taylor[14] shows that TNT should be twice as effective as a blast or kinetic energy producer as the same amount of energy released at a point in air. In rocket nozzles the energy added by the drag per unit mass of injectant is of the same order as the energy per pound of TNT, and thus similar increases in effectiveness can be expected in this case. Hence the two new effects are approximately equal in magnitude but opposite in sign and are, for the present purposes, ignored. This point is worth further consideration, however, especially in the comparison of results from hot and cold nozzle flow tests where the energy per pound of injectant differs considerably.

‡‡ The analysis of Shapiro[12] shows that the addition of mass with zero momentum to flow in a pipe is duplicated exactly by this scheme, provided only that the total temperature of the injectant is the same in the two cases. This does not constitute a proof, but the result is pertinent.

References

[1] Newton, J. F., Jr. and Spaid, F. W., "Interaction of secondary injectants and rocket exhaust for thrust vector control," ARS J. **32**, 1203–1211 (1962).

[2] Lees, L. and Kubota, T., "Inviscid hypersonic flow over blunt-nosed slender bodies," J. Aerospace Sci. **24**, 195–202(1957).

[3] Wu, J.-M., Chapkis, R. L., and Mager, A., "Approximate analysis of thrust vector control by fluid injection," ARS J. **31**, 1677–1685 (1961).

[4] Ferrari, C., "Interference between a jet issuing laterally from a body and the enveloping supersonic stream," Bumblebee Series Rept. 286, Appl. Phys. Lab., Johns Hopkins Univ. (April 1959).

[5] Sakurai, A., "On the propagation and structure of the blast wave, I," J. Phys. Soc. Japan **8**, 662–669 (1953).

[6] Sedov, L. I., *Similarity and Dimensional Methods in Mechanics* (Academic Press, New York and London, 1959), Chap. IV.

[7] Sakurai, A., "On the propagation and structure of a blast wave, II," J. Phys. Soc. Japan **9**, 256–266 (1954).

[8] Rodriguez, C. J., "An experimental investigation of jet-induced thrust vector control methods," Bull. 17th Annual JANAF-ARPA-NASA Solid Propellant Meeting, Vol. III, Johns Hopkins Univ., Appl. Phys. Lab., pp. 77–122 (September 1961).

[9] Amick, J. L. and Hays, P. B., "Interaction effects of side jets issuing from flat plates and cylinders aligned with a supersonic stream," Wright Air Div. Div. TR 60-329 (June 1960).

[10] Broadwell, J. E., "An analysis of the fluid mechanics of secondary injection for thrust vector control (revised)," Space Technology Labs. Inc., Rept. 6120-7744-MU-000 (March 15, 1962).

[11] Walker, R. E., Stone, A. R., and Shandor, M., "Secondary gas injection in a conical rocket nozzle, 1: Effect of orifice diameter and molecular weight of injectant," Johns Hopkins Univ., Appl. Phys. Lab. Rept. CM-1010 (February 1962).

[12] Shapiro, A. H., *The Dynamics and Thermodynamics of Compressible Flow* (The Ronald Press Co., New York, 1953), Vol. I, Chap. 8.

[13] Willmarth, W. W., "The production of aerodynamic forces by heat addition on external surfaces of aircraft," Rand Corp. Res. Memo. RM-2078 (December 30, 1957).

[14] Taylor, G. I., "The formation of a blast wave by a very intense explosion, I: Theoretical discussion," Proc. Roy. Soc. (London) **A201**, 159–174 (1950).

[15] Amick, J. L., private communication (January 2, 1962).